Tribology International 80 (2014) 1–6

Contents lists available at ScienceDirect

Tribology International

journal homepage: www.elsevier.com/locate/triboint

Short Communication

Seizure pressure and sliding velocity diagrams on tribological behavior of Al alloy composites in as-cast and heat-treated conditions

R.N. Rao [a,*], S. Das [b], S.L. Tulasi Devi [c]

[a] Mechanical Engineering Department, National Institute of Technology, Warangal-506 004, Andhrapradesh, India
[b] Advanced Materials and Processes Research Institute (CSIR, New Delhi), Bhopal-462 026, India
[c] SOM, National Institute of Technology, Warangal-506 004, Andhrapradesh, India

ARTICLE INFO

Article history:
Received 16 March 2014
Received in revised form
30 May 2014
Accepted 12 June 2014
Available online 23 June 2014

Keywords:
Aluminium alloy
Seizure pressure
Sliding velocity
Wear mechanism

ABSTRACT

The conventional way of rating the performance of a material subjected to sliding wear is in the form of *P–V* diagram. The seizing of material is due to changing in the elastic limit and flow stress due to thermal softening and in due course due to cold welding in localized region between the two surfaces. Because of these interactions the allowable pressure decreases with increase in velocity and vice versa. It is to be observed that simply by heat treatment of alloy the seizure resistance is enhanced by 12.5% and further 22.2% by dispersion of 10 wt% of SiCp to alloy. All these facts are discussed on the basis of prevailing wear mechanism.

1. Introduction

Metal matrix composites especially aluminium matrix composites have been emerged as advanced materials for several potential applications in defence, automobile, aerospace, aircraft and other engineering sectors because of their high specific strength and stiffness, superior wear and seizure resistance as compared to the alloy irrespective of applied load and sliding speed [1–6]. Attempts have been made to examine the Seizure pressure as a function of sliding velocity on tribological behavior of Al-SiC composites in as-cast and heat-treated conditions. A systematic approach to examine wear phenomena and transitions in wear mechanism over wide ranges of load and sliding speed was first adopted by Welsh in studies of the sliding wear of mild steel [7]. Empirical wear maps in which these effects are summarized as a function of load and sliding speed offer a convenient means for predicting and understanding dry sliding wear behavior. Such approaches have been adopted for steel-on-steel sliding and other material combinations have been applied successfully to aluminium alloys [8–11]. Several investigators [12,13] adopted a similar approach to using wear rate and wear mechanism data for aluminium alloys. While aluminium alloys sliding against steels, several wear mechanisms were identified such as oxidation-dominated wear, delamination wear, severe plastic deformation wear, seizure and melt wear. The dominant mechanism can be plotted on normalized pressure and velocity axes. Rohatgi et al. [14] clearly demonstrated the influence of graphite content on critical conditions for seizure in dry sliding against steel for Al–Si–graphite composites and also Al–12% Si and Al–Si–Cu (LM30) Al alloys. The seizure behavior is summarized in a plot of normalized velocity and pressure. Graphite additions to MMCs produce similar enhancements in seizure resistance [15]. According to these investigators [16–21] four wear regimes were observed in the composites and the alloy depending on speed and applied load. They are mild wear, mixing and oxidative wear, delamination wear and severe wear. Aluminium silicon alloys exhibit several features of tribological behavior which are similar to those of aluminium-based MMCs. The effect of silicon content in Al–Si alloys in dry sliding wear has summarized by Zum Gahr [22]. Wear resistance is improved in mild wear conditions, if the silicon content in Al–Si alloys is increased. The wear resistance of each alloy is increased with primary silicon content up to a maximum at 17% Si. A transition load at which wear rates changed from mild to severe was also identified for different silicon contents and sliding speeds. Based on data from Andrews et al. [23] a load velocity diagram is plotted, that indicates the beneficial effect of silicon content on resistance to severe wear. The onset of severe wear occurred at a characteristic transition load, at which a small

* Corresponding author. Tel.: +91 9441569066; fax: +91 8702459547.
E-mail addresses: rnraonitw@gmail.com, rnrao@nitw.ac.in (R.N. Rao).

http://dx.doi.org/10.1016/j.triboint.2014.06.007
0301-679X/

quantity of aluminium adhered to the steel disk. This transferred deposit grew in size and initiated gross plastic deformation and fracture of the aluminium alloy pin as the test progressed. Material removal occurred by subsurface crack propagation in a composite transfer layer of aluminium and crushed silicon particles during mild wear and by subsurface cracking at silicon particles in the highly deformed wear zone during severe wear.

Numerous investigations of the dry sliding wear of aluminium matrix composites against steels have reported significant increases in their wear resistance compared with unreinforced aluminum alloys. When contact loads and sling speed are kept very low, so that frictional heating effects are negligible, ceramic reinforcing particles tend to support the contact stresses. Subsurface plastic deformation and shear of the matrix alloy is prevented by the constraint introduced by the reinforcing phase. Sliding wear tests of 6061 Al–20 vol% Al_2O_3 against SAE 52100 bearing steel, the load support provided by particulate reinforcement in ultra mild wear demonstrated by Zhang and Alpas [24]. During sliding the exposed portions of Al_2O_3 particulates created a local abrasive action on the steel counter surface. The worn steel fragments were transferred to the composite surface to form a protective, ion-rich transfer layer which tended to oxidize, producing a reddish brown Fe_2O_3 wear scar. Iron oxide shows a low coefficient of friction in sliding against steel and thus the transfer layer provided an in situ lubricating effect. The transition wear behavior of SiC particulate and SiC whisker-reinforced 7091 Al alloys at a constant contact load of 13 N studied by Wang and Rack [25]. At sliding velocities below 1.2 m/s the wear rates of unreinforced 7091 Al and the 20 vol% SiCp and SiCw reinforced 7091 Al MMCs were of similar magnitude. Zhang and Alpas [26]; Wilson and Alpas [20] demonstrated the wear debris by both the composites and the unreinforced alloy below 1.2 m/s was dark in colour and consisted of fine, equiaxed, predominantly metallic particulates, typical of that seen in the mechanical mixing/oxidation regime for aluminium alloys. Wang and Rack [27] suggested that the mechanism of wear under these conditions resulted from cracking by surface fatigue to produce the small metallic debris particles. Wang and Rack [25] is also studied the effect of sliding velocity on the wear of unreinforced 7091 Al and MMCs reinforced with SiC particulates and whiskers, above 1.2 m/s in their experiments, the wear rates of the MMCs tended to be lower than that of 7091 Al; the debris produced was flake chip like in morphology for both sets of materials. The wear behavior above 1.2 m/s was termed severe in that transfer to the counter face of debris was found, accompanied by severe cracking and plastic deformation to the subsurface worn region and metal-to-metal contact. Modi et al. [28] studied particulate additions to the Al alloys provide improved resistance to severe wear and seizure. Enhanced seizure resistance, compared with the unreinforced alloy, has been observed in Al–4.5% Cu alloy (LM11) MMCs reinforced with 10 vol% of SiC particulates and 10 vol% of SiC fibres, respectively. Rohatgi et al. [29] demonstrated the influence of graphite on seizure resistance in Al–12% Si and Al–Si–Cu (LM30) Al alloys and the seizure behavior is summarized in a plot of normalized velocity and pressure.

In view of the above, in the present study tribological behavior of aluminium matrix composite has been examined under specific applied pressure and sliding speed. Identifying the critical load and sliding speed for transition of one wear mechanism to other gives the rating performance of a material subjected to sliding.

2. Materials and methods

2.1. Material preparation

Aluminium matrix composite was synthesized through solidification processing (stir-casting) route using AA7010, AA7009 and AA2024 alloy as matrix and SiC particle (size range: 20–40 μm, wt %: 10, 15 and 25) in the present study. The alloy had a chemical composition of Fe-0.27%, Cu-1.28%, Mg-1.14, Zn-5.30% and Al-rest. The composite and the alloy were cast in the form of cylinders of dimension: 200 mm in length and 16 mm in diameter, in a permanent cast iron die. The cast samples were mechanically polished and etched with Keller's reagent (1% HF, 1.5% HCl, 2.5% HNO_3 and remaining water) for microstructural and wear surface observations in SEM (model: JEOL, JSM-5600). The etched samples were sputtered with gold prior to SEM examination.

2.2. Sliding wear tests

Dry sliding wear tests of the alloy and its composites in as-cast and heat-treated containing 10,15 and 25 wt% SiC particles were carried out using a DUCOM (India) make pin-on-disc machine (Model: TR 2O LE). Cylindrical test pins (8 mm diameter and 27 mm length) were held against a rotating heat-treated EN32 steel disc conforming to AISI 52100 (1.0%C, 1.4%Cr, 0.40%Mn, 0.2% Si, 0.05%S, 0.05%P and remainder Fe). Hardness of the disc was 65 HRC. The steel disc and the samples were polished mechanically up to a roughness (Ra) value of 0.10 μm prior to each test. Wear tests were conducted over a range of applied pressures and sliding speeds. The track diameter of 100 mm, sliding velocities of 0.52, 1.72, 3.35, 4.18 and 5.2 m/s, respectively were used. Load on the specimen was increased in steps until the specimen seized. Seizure of the specimen was noticed in terms of large material adhesion on to the disc, higher rate of temperature rise of the test pin, and abnormal vibration and noise from the pin-on-disc assembly. Frictional heating was monitored using a chromel–alumel thermocouple inserted in a 1.5 mm diameter hole on the test pin, 1.5 mm away from the sliding surface. The samples were cleaned with acetone and weighed (accuracy of 0.01 mg) prior to and after each test. A set of three samples was tested in every experimental condition and their average value is reported. A Mettler microbalance (Model: H15AR) was used for weighing the specimens. Weight loss was then converted into volume loss per unit sliding distance to compute wear rate.

3. Results and discussion

A typical scanning electron micrograph of SiC particles shows morphology of particle in Fig. 1(a). It may be noted that the particles are of in-equiaxed nature, with sharp corners Fig. 1(b). A higher magnification micrograph of SiC particles clearly depicts morphological structure of sharp edged and equiaxed SiC particles Fig. 1(c). A typical scanning electron micrograph of Al–Zn–Mg–Cu (AA7010) alloy consists of dendrites of Al and precipitates along the interdendritic regions Fig. 1(d). A typical scanning electron micrograph of Al–Zn–Mg–Cu heat-treated alloy shows the aluminium phase (black) in colour and precipitates (white) in colour distributed in the Al matrix Fig. 1(e). A higher magnification micrograph of Al–Zn–Mg–Cu clearly shows the formation of precipitates found the Al matrix. The morphology of the precipitates varies from equiaxed to lamellar. The equiaxed precipitates are of 2–5 μm in size. The lamellar precipitates are usually are of around 10–15 μm in length, and 2–3 μm in width. As per as composite concerned, other composites are also same material combinations having different percentage of SiC. Hence the nature of SiC distribution is same with different densities.

Fig. 2(a) represents the seizure pressure as a function of sliding velocity for 7010 alloy and composites in as-cast and heat-treated conditions. This figure demonstrates seizure pressure decreases with increase in sliding velocity and the heat treatment has no significant influence on seizure pressure, especially at higher velocity (>1.72 m/s). For example the seizure pressures of as-

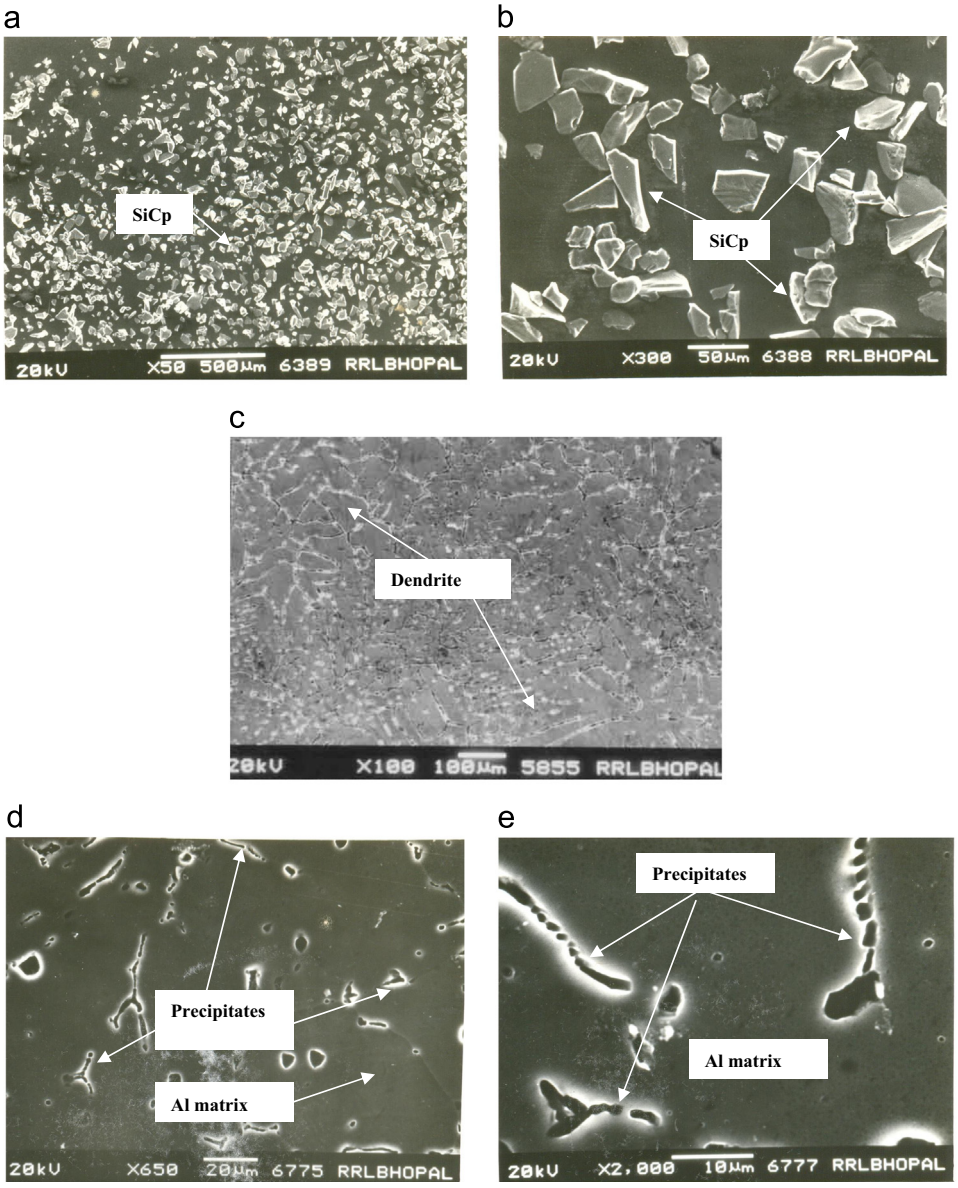

Fig. 1. A typical scanning electron micrograph of (a) SiC particles, (b) higher magnification SiC particles, (c) as cast Al–Zn–Mg–Cu alloy, (d) heat-treated alloy, (e) higher magnification heat-treated alloy. (For interpretation of the references to colour in this figure legend, the reader is referred to the web version of this article.)

cast 7010 alloy, at sliding velocity of 0.52, and 1.72 m/s, are noted to be 2.60 MPa and 2.00 MPa respectively. Further increasing sliding velocity to 3.35 m/s leads to decreasing seizure pressure to 1.6 MPa. When the sliding velocity increase to 5.23 m/s the seizure pressure of as-cast 7010 alloy reduced further to 0.8 MPa. The seizure pressure of heat treated 7010 alloy at sliding velocity of 0.52 m/s and 1.72 m/s are noted to be 2.8 and 2.2 MPa respectively, which are greater than that obtained in as-cast condition. The seizure pressure of 7010 alloy is noted to be same as that of as-cast alloy when the sliding velocity is 3.35 m/s or more. Similarly for 7010-25 wt% SiC reinforced composite in as-cast condition, the seizure pressures at sliding velocity of 0.52, 1.72, 3.35, 4.18 and 5.23 m/s are noted to be 3.4, 2.8, 2.6, 1.6 and 1.2 MPa respectively. In the case of heat treated 7010–25 wt% SiC reinforced composite, the seizure pressures at sliding velocity of 0.52 and 1.72 m/s are noted to be 3.6 and 3.0 MPa respectively. At higher sliding velocity ($\geq$ 3.35 m/s) the as-cast and heat-treated composites exhibited the same seizure pressure. Similar types of trend were observed for Al-10 wt% and Al-15 wt% SiC reinforced composite.

Fig. 2(b) depicts the seizure pressure as a function of sliding velocity for 7009 alloy and composites in as-cast and heat-treated conditions. It is evident from the figure that the seizure pressure decreases with increasing sliding velocity irrespective of material. In case of composites seizure pressure increases with increasing SiC content irrespective of sliding velocity. It is further noted that at higher sliding velocity, the seizure pressure of a material does not improve due to heat treatment, whereas at lower sliding velocity material exhibited marginally higher seizure pressure in heat-treated condition as compared to that in as-cast condition. For example, the seizure pressure of the alloy at sliding velocity of 0.52, 1.72 and 3.35 m/s are noted to be 2.2, 1.6 respectively in as-cast condition. When the sliding velocity increases to 4.18 and 5.23 m/s, the seizure pressures decreases to 1.0 and 0.6 MPa respectively. In the case of heat-treated alloy, the seizure pressure at sliding velocity of 0.52, 1.72, and 3.35 m/s are noted to be 2.4, 1.8 and 1.6 MPa, which are higher than by 0.2 MPa as compared to the as-cast one. However, when the sliding velocity reaches to 4.18 m/s the seizure pressure of heat-treated alloy also noted be 1.0 MPa, which is same as that of as-cast one. In the case of 7009–

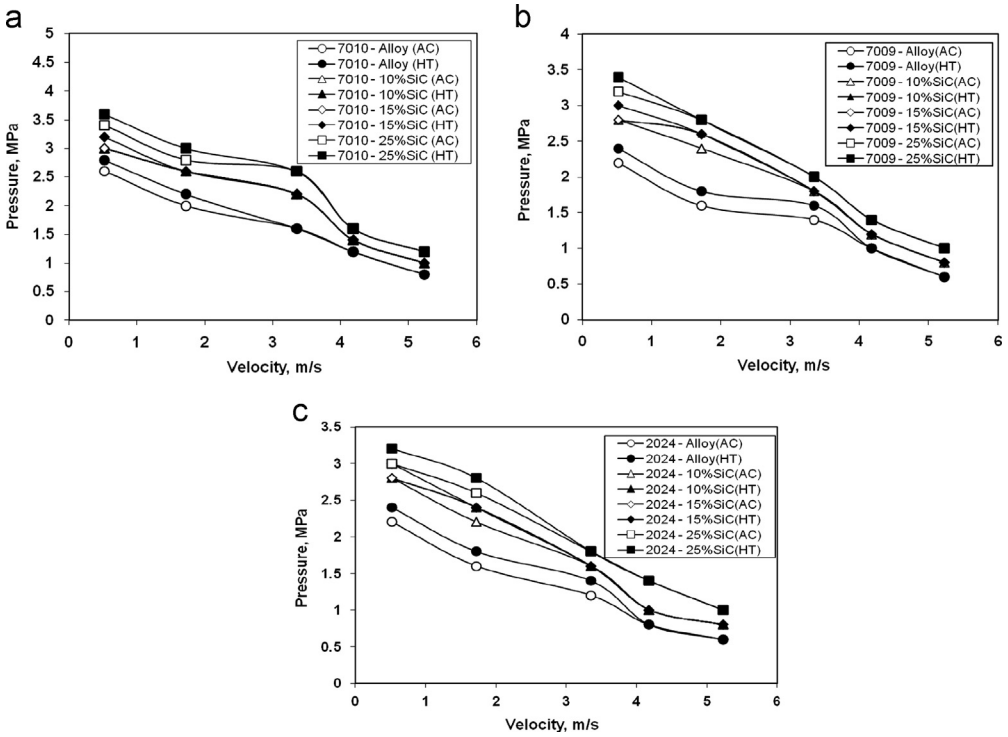

Fig. 2. Pressure-velocity limits of (a) AA7010 alloy and composites; (b) AA7009 alloy and composites; (c) AA2024 alloy and composites.

25 wt% SiC composite, the seizure pressure in as-cast and in heat-treated condition at the sliding velocity of 0.52 m/s are noted to be 3.4 and 3.2 MPa respectively. But when the sliding velocity increase to 1.72 m/s or more, the seizure pressure of 25 wt% SiC reinforced composite in both as-cast and heat-treated condition noted to be same. Similar trend is noted to for 10 and 15 wt% SiC reinforced composite.

The seizure pressure as a function of sliding velocity for 2024 alloy and composites in as-cast and heat-treated conditions are depicted in Fig. 2(c). It is evident from the figure that seizure pressure is decreases with increasing sliding velocity and increases with increasing SiC content, as was observed in earlier Fig. 2(a) and (b) for 7010 and 7009 alloy and composites. It is further noted that the lower sliding speed the seizure pressure of the materials improved due to heat treatment. At higher sliding velocity, the seizure pressure of the materials is noted to be same in as-cast and in heat-treated conditions. For example, in the case of 2024 alloy the seizure pressure at sliding velocity of 0.52, 1.72 and 3.35 m/s in as-cast condition are noted to be 2.2, 1.6, and 1.2 MPa, respectively, and in heat-treated condition at 2.4, 1.8 and 1.4 MPa, respectively. When the sliding velocity increases to 4.18 and 5.23 m/s, the seizure pressure of the alloy in both as-cast and heat-treated conditions reduces to 0.8 and 0.6 MPa, respectively. Similarly for 2024–25 wt% SiC reinforced composites, the seizures at sliding velocity of 0.52 and 1.72 m/s in as-cast condition are noted to be 3.0 and 2.6 MPa respectively.

It is noted that the seizure pressure of 7010 alloy is higher than that of 7009 and 2024 alloy irrespective of sliding velocity. However, in the case of 2024 and 7009 alloy, the seizure pressure at lower velocity (0.52, 1.72 m/s) is noted to be almost same and this fact is also true for higher velocity 5.23 m/s. At an intermediate velocity (3.35, 4.18 /s), the seizure pressure of 7009 alloy is noted to be higher than that of 2024. Performance wise the alloy system may be arranged in the following order 7010 > 7009 > 2024 alloy. It is to be observed that simply by heat treatment of alloy, the seizure resistance is enhanced by 12.5%, and by dispersion of 10% weight of SiC particles, the seizure resistance is increased by 22.2%. Further, the seizure resistance is increased by 30% by dispersion of 25% weight of SiC particles. Hence, as per the experimentation and results, 25 wt% SiC reinforced composite gives best results and more wear resistance than that of alloy.

Fig. 3(a) shows a higher magnification micrograph of wear surface of alloy at an applied pressure of 1.0 MPa alloy, and clearly depicts the cracks propagating along the longitudinal as well as transverse directions (arrow marked) and also observed damaged region from which the portion of the top surface is detached. Micrograph of wear surface of seized alloy is characterized by the formation of parallel lips along the groove markings in Fig. 3(b). A higher magnification micrograph of wear surface of 25 wt% SiC reinforced composite at an applied pressure of 1.8 MPa, clearly indicates damaged portion in which the debris are formed mainly due to the high deformation and tearing action and chunky mass are formed as debris in Fig. 3(c). Micrograph of wear surface of 25 wt% SiC composite seized at an applied pressure of 2.0 MPa and the wear surface is characterized by the formation of parallel lips along the wear scar in Fig. 3(d).

An attempt has been made to analyze the results expressed by Archard's wear Eq. (1), the wear rate of a material is directly influence by external variables, such as load, sliding distance, and sliding velocity. Wear rate evaluated using a wear equation based on the work of Archard [30] is given by

$$Q = KW/H \tag{1}$$

where Q is the volume removed from the surface by wear per unit sliding distance, H the indentation hardness of the softer surface, W the normal pressure applied between the surface and K the Archard's wear coefficient is dimensionless always less than unity. The value of K provides valuable means of comparing severity of different wear processes. For sliding wear of metals typical values of K for the mild wear of metals are 10^{-4} to 10^{-6}, while K becomes 10^{-3} to 10^{-2} for severe wear.

Several wear mechanisms have been reported in studies of Al and its alloys in dry sliding contact against steel surfaces. They identified two wear mechanisms in aluminium alloys: one oxidational and the other metallic. Sliding wear of Al alloy is mainly

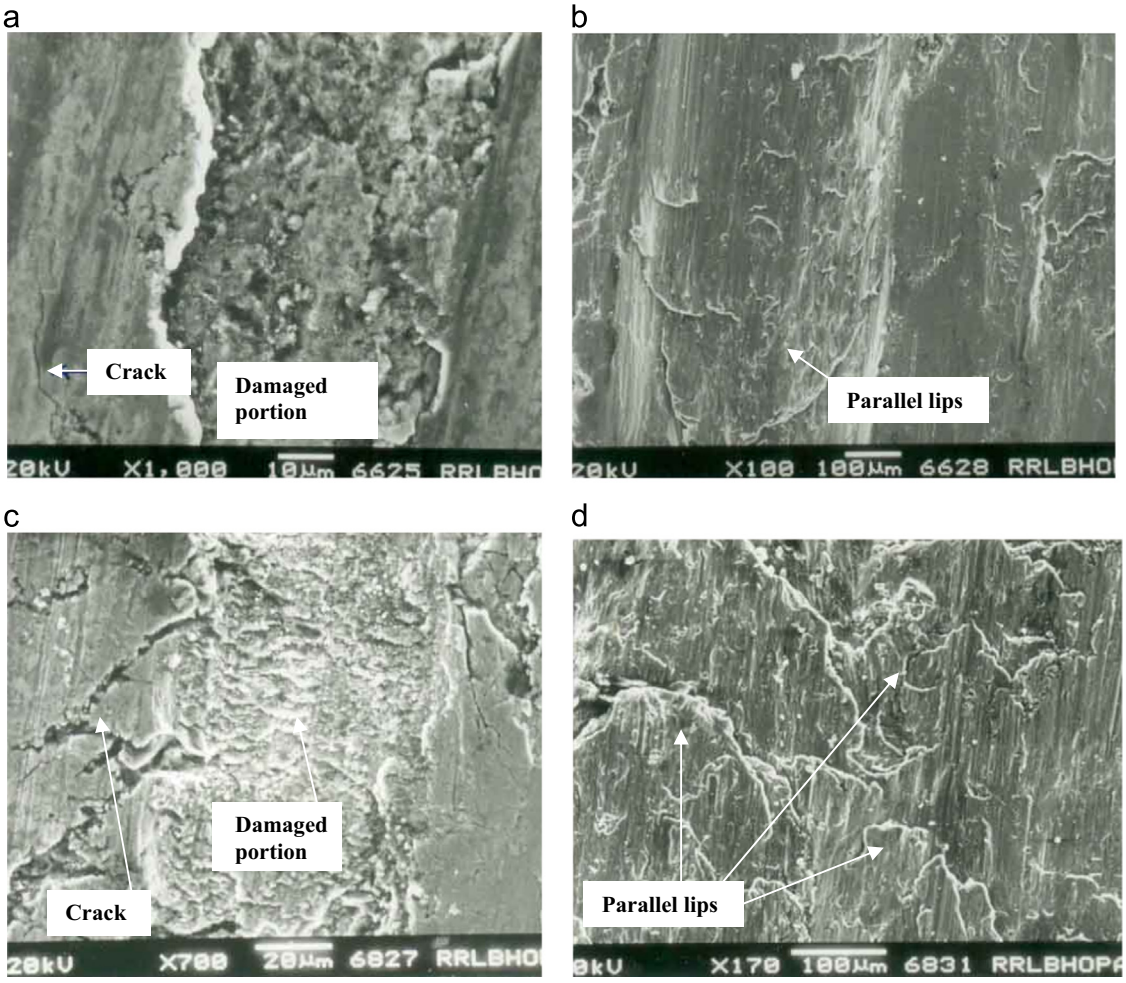

Fig. 3. Typical scanning electron micrograph of worn surface of (a) alloy at higher applied pressure (b) alloy at seizure pressure (c) 25 wt% SiC reinforced composite at higher applied pressure and (d) 25 wt% SiC reinforced composite at seizure pressure.

governed by the two types of wear situations, namely, the mild and severe wear. In the mild wear regime, the oxide layer is removed, once the oxide layer is removed, the fresh surface is exposed out and severe wear takes place essentially due to adhesion followed by delamination. In the case of composite, in the initial stage of sliding, aluminium is worn out exposing SiCp. The protruded SiC particles come directly into contact with the disc and resist further wear of material. At higher applied pressure, there is every possibility that the crack will be nucleated at the interfaces of matrix and reinforcement. In such a situation, the crack propagates along the interfaces and joins together to form a chunky mass of material which may come out of the sample and resulted in higher wear rate. At lower pressure, the debris was dark and powdery, and at higher pressure, the debris become metallic and flake shaped. For lower pressure, it was observed that parallel and continuous grooves are formed, whereas at higher pressure, delamination wear predominant. The severity of surface damage increased with pressure.

The performance rating of the material subjected to sliding wear is in the form of *P*–*V* diagram, which indicate the maximum allowable pressure (*P*) at a specific velocity (*V*) or vice versa the material can withstand. The seizing of material is due to changing in the elastic limit, and flow stress due to thermal softening and in due course due to cold welding in localized region between the two surfaces. The cold welding is a function of effective temperature on the surface, which is again function of pressure and velocity and their interaction. Increase in pressure leads to more surface contact and thus increase in frictional force, which leads to increasing in temperature. Once again increase in velocity leads to less temperature and less degree of heat transfer and more adiabatic heating. As a result there is an interaction between velocity and pressure, which results in more temperature rise and possibility of cold welding in the localized region. Because of these interactions the allowable pressure decreases with increase in velocity and vice versa.

4. Conclusions

1. The rating of the performance of a material subjected to sliding wear in the form of *P*–*V* diagram.
2. It is evident from the figures that the allowable pressure decreases with increasing sliding velocity irrespective of material but reverse is true in the case of heat-treated conditions.
3. It is further noted that heat treatment has no significant influence on seizure pressure especially at higher pressure.
4. Performance wise the alloy system may be arrange in the form of 7010 > 7009 > 2014.
5. It is noted that the measured values are in good agreement with the theoretically calculated value.
6. Simply by heat treatment of alloy, the seizure resistance is enhanced by 12.5%, and by dispersion of 25 wt% SiCp, the seizure resistance is increased by 30%.

7. The wear surface of alloy depicts the cracks propagating along the longitudinal as well as transverse directions and seized sample is characterized by the formation of parallel lips along the wear scar.

References

[1] Rohatgi PK. Metal matrix composites. J Def Sci 1993;43:323–49.
[2] Nussbaum AI. New applications for aluminium based metal matrix composites. Light Metal Age 1997:54–8.
[3] Mondal DP, Das S, Rao RN, Singh M. Effect of SiC addition and running-in-wear on the sliding wear behaviour of Al–Zn–Mg aluminium alloy. Mater Sci Eng, A 2005;40(1-2):307–19.
[4] Rao RN, Das S, Mondal DP, Dixit G. Dry sliding wear behaviour of cast high strength aluminium alloy (Al–Zn–Mg) and hard particle composites. Wear 2009;267:1688–95.
[5] Qin QD, Zhao YG, Zhou W. Dry sliding wear behavior of Mg_2Si/Al composites against automobile friction material. Wear 2008;264:654–61.
[6] Mandal A, Murty BS, Chakraborty M. Sliding wear behaviour of T6 treated A356–TiB_2 in-situ composites. Wear 2009;266:865–72.
[7] Welsh NC. The dry sliding of steels. Philos Trans R Soc London, Ser A 1965;257:31–50.
[8] Lim SC, Ahsby MF. Wear-mechanism maps. Acta Metall 1987;35:1–24.
[9] Ashby MF, Abhulawi J, Kong HS. Temperature maps for frictional heating in dry sliding. Tribol Trans 1991;34:577–87.
[10] Kato H, Eyre TS, Ralph B. Wear mechanism map of nitrided steel. Acta Metall Mater 1994;42:1703–13.
[11] Hsu SM, Lim DS, Wang YS, Munro RG. Ceramics wear maps: concept and method development. Lubr Eng 1991;47:49–54.
[12] Antoniou R, Subramanian C. Wear mechanism map for aluminium alloys. Scr Metall 1998;22:809–14.
[13] Rao RN, Das S, Mondal DP, Dixit G, Tulasi Devi SL. Dry sliding wear maps for AA7010 (Al–Zn–Mg–Cu) aluminium. Tribol Int 2013;60:77–82.
[14] Rohatgi PK, Liu Y, Asthana R. Tribology of composite materials. In: Rohtagi PK, Blau PJ, Yust CS, editors. Novelty, OH: ASM International; 1990. p. 69–79.
[15] Lin JF, Yung YC, Tsao CY. Tribological performance of 6061 aluminum alloy/graphite materials under oil-lubricated and dry sliding conditions. Tribol Trans 1998;41:251–61.
[16] Wilson S, Alpas AT. Wear mechanism maps for metal matrix composites. Wear 1997;212:41–9.
[17] Lim SC, Ashby MF. Wear mechanism maps. Acta Metal 1987;35(1):1–24.
[18] Rao RN, Das S, Mondal DP, Dixit G. Mechanism of material removal during tribological behaviour of aluminium matrix (Al–Zn–Mg–Cu) composites. Tribol Int 2012;53:179–84.
[19] Lim SC, Ashby MF, Brunton JH. Wear-rate transitions and their relationship to wear mechanisms. Acta Metall 1987;35:1343–8.
[20] Wilson S, Alpas AT. Thermal effects on mild wear transitions in dry sliding of an aluminium alloy. Wear 1999;225-229:440–9.
[21] Chen H, Alpas AT. Sliding wear map for the magnesium alloy, Mg–9Al–0.9Zn (AZ91). Wear 2000;246:106–16.
[22] Zum Gahr KH. Microstructure and wear of materials. Tribol Ser 1997:10.
[23] Andrews JB, Seneviratne MV, Zeir KP, Jett TR. Proc Conf Wear Mater 1985180–5 (1985).
[24] Zhang J, Alpas AT. Wear regimes and transitions in $A1_2O_3$ particulate-reinforced aluminium alloys. Mater Sci Eng 1993;A160:25–35.
[25] Wang AG, Rack HJ. Transition wear of Al metal matrix composites. Mater Sci Eng 1991;A147:211–24.
[26] Zhang J, Alpas AT. Transition between mild and severe wear in aluminum alloys. Acta Mater 1997;45:513–28.
[27] Wang AG, Rack HJ. Abraisve wear of silicon carbide particulate and whisker-reinforced 7091 aluminium matrix composites. Wear 1991;146:337–48.
[28] Modi OP, Prasad BK, Yegneswaran, Vidya ML. Corrosion behaviour of squeeze-cast aluminium alloy-silicon carbide composites. Mater Sci Eng 1992; A151:235–45.
[29] Rohatgi PK, Liu Y, Lim SC. Wear mapping for metal and ceramic matrix composites. Adv Compos Tribol 1993291–309.
[30] Archard JF. Contact and rubbing of flat surfaces. J Appl Phys 1953;24:981–8.